ELSEVIER

Journal of Nuclear Materials 271&272 (1999) 333–339

journal of nuclear materials

Behavior of ion-implanted helium and structural changes in nickel-base alloys under long-time exposure at elevated temperatures

I.I. Chernov *, B.A. Kalin, A.N. Kalashnikov, V.M. Ananin

Moscow State Engineering Physics Institute (Technical University), 31 Kashirskoye sh., Moscow 115409, Russian Federation

Abstract

The regularities of helium trapping and release and structural changes in the model alloys of a Ni–Al system after post-irradiation annealings at 920–1120 K up to 25 h have been studied by means of thermodesorption spectrometry (TDS), internal friction (IF) measurement and transmission electron microscopy (TEM). The samples were irradiated by He^+-ions at room temperature up to fluence of 5×10^{20} m^{-2}. It was shown that the quantity of helium remaining in Ni is considerably less than in solid solutions after long-time post-irradiation annealing at 1020 and 1070 K. The IF measurements showed that irradiation resulted in the formation of additional peaks in the IF spectra which were not detected in the IF spectra of unirradiated samples. The obtained data give grounds to propose that more thermally stable complexes containing vacancies, helium and alloying element atoms (complexes of $He_mAl_kV_n$ type) can be formed in the substitutional solid solutions along with usual complexes of He_mV_n type in pure nickel.

1. Introduction

Along with a high degree of radiation damage of materials structure a significant quantity of helium will be accumulated within the fusion reactors first wall and blanket materials via (n, α) or other transmutation reactions as well as it may be implanted from plasma through the first wall material surfaces unprotected against radiation [1,2].

Helium can have a pronounced effect on the radiation damaging of materials and often may be an important reason in catastrophic degradation of their properties and shortening of the useful life of reactor constructional elements [1–4]. Such effects are: stabilization of vacancy agglomerates by gas atoms and dramatic impact on the kinetics of radiation swelling [1–6]; role of helium in the high-temperature grain boundary radiation embrittlement (HTRE) [1–4,7], in particular, the effect of HTRE and stability of helium-vacancy complexes may be interdependent as was shown in [6].

As shown earlier [8,9], a different quantity of pre-implanted helium remains in the alloys of Ni–Al and Ni–Ti systems after long-time post-irradiation annealing (25 h, 1020 K). It was proposed that this effect is induced by formation of more thermally stable complexes of $He_mM_kV_n$ type (He is atom of helium; M, atom of Al or Ti; V, vacancy) in the substitutional solid solutions along with usual complexes of He_mV_n type in pure nickel.

The aim of this paper is to check this speculation and to obtain the temperature range of these complicated complexes existence using an estimation of the total quantity of helium remaining in the alloys after post-irradiation annealing at 920–1120 K as well as using the IF measurements of irradiated alloys and investigation of the sample fine structure by TEM.

2. Experimental procedure

The Ni–Al system binary alloys (with aluminum concentration $N_{Al} = 0$–7.5 wt%) were prepared from high-purity Ni and Al (99.999%) according to the technique described earlier [10]. After repeated rolling with

* Corresponding author. Tel.: +7-095 323 92 72; fax: +7-095 323 31 65; e-mail: chernov@phm.mephi.ru

0022-3115/99/$ – see front matter
PII: S0022-3115(98)00718-1

intermediate homogenizing annealings to final thickness of 0.2 mm they were quenched into iced water from 1370 K after their exposure for 1 h.

The electropolished samples $55 \times 5 \times 0.2$ mm^3 sized were irradiated under identical conditions (in a special cartridge) by surface scanning 40-keV helium ions up to a fluence of 5×10^{20} m^{-2} at room temperature. The microstructural investigations were performed in TEM JEOL-200CX. The details of trapping and release of implanted helium were studied by means of a helium partial pressure meter [11]. The internal friction (IF) was measured using a type straight pendulum apparatus by means of bend damping out oscillations of cantilever clamped plate samples. The inclination tangent of a linear part of amplitude-independent IF on the plots of A_i versus N_i (N_i is the sample vibration number) defines the IF value. The estimated ranges of measuring the IF values were from 5×10^{-4} up to 120×10^{-4} for vibration frequencies 0.5–15 Hz with the mean relatively error about 0.9% for four sets of experiments.

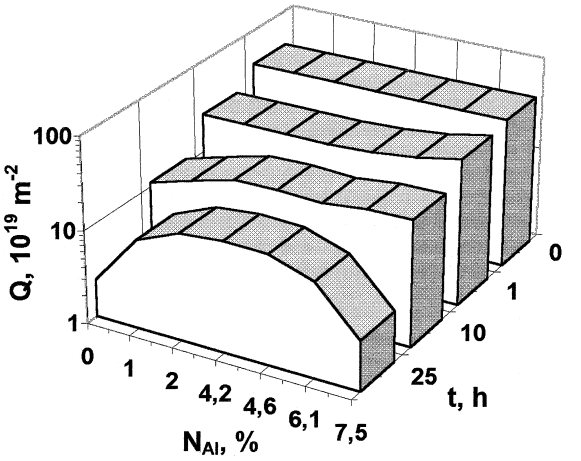

Fig. 1. The amount of helium remained in Ni–Al alloys after post-irradiation annealing at 1020 K in dependence on Al content and annealing time.

3. Results

Post-irradiation annealings for 1 h and even for 10 h at 920 K do not involve detectable changes in the quantity of initially implanted helium.

The dopant concentration significantly influences the quantity of gas remaining in samples *annealed at 1020 K* (Fig. 1). With increasing of annealing time the total concentration of helium decreases in all alloys, but for pure Ni and decomposing alloys ($N_{Al} > 5\%$) it decreases much more than for solid solutions, so that in solid solutions of Al in Ni the quantity of retained helium is up to 30–40% of initially trapped helium content, that is essentially higher than that of gas remained both in pure Ni and decomposing alloy of Ni–7.5%Al (about 5–7% only) after 25 h annealing.

Post-irradiation annealing up to 10 h at 1070 K causes helium to remain in the alloys about 1.5 times greater than its content in pure nickel, gas release takes place in the more width temperature range and the TDS peaks shift significantly to a higher temperature region for alloy than those fore pure nickel (Fig. 2). The large bubbles are formed after annealing at this temperature (see Table 1 and Fig. 3).

Almost the whole pre-injected helium released from all specimens after *post-irradiation annealing during 25 h at 1120 K*. TEM showed and calculations supported [12] that implanted helium released by bubble migration and coalescence forming a chain of channels in the near-surface sample structure and pin-hole structure on its surface (Fig. 3(c) and (d)).

The typical TEM-images of irradiated samples and the bubble parameters formed after various regimes of annealing are presented in Fig. 3 and in Table 1. The role of alloying elements (Al and Ti in Ni) in the bubble evolution process during post-irradiation annealing up to 25 h at 1020 K has been studied in details in Refs. [8,9,13,14].

As can be seen from the present results and data presented earlier [8,9,13,14], the size of bubbles reduces and their density grows with an increase of Al concentration in Ni. However annealings at 1020 and 1070 K during 10 h or more violate the regularity in decomposing alloys. For example, two systems of bubbles form in alloy Ni–7.5%Al: fine bubbles which are located in grains and on dislocation lines, and large bubbles connected with particles of the secondary γ'-Ni_3Al phase (Fig. 3(b)). At the expense of that, the average bubble size grows and the bubble density decreases (Table 1).

Very large pores with $d > 150$ nm penetrating the irradiated layer and crossing the sample surface are formed after annealing for an 25 h at 1120 K. Thus as

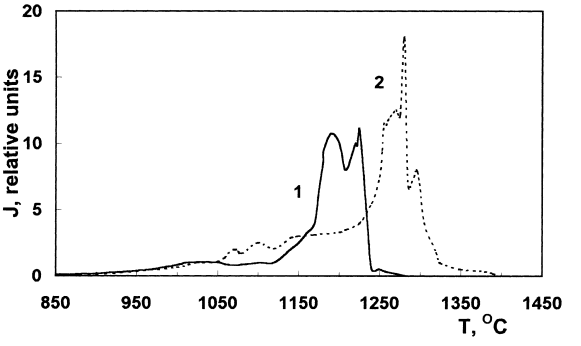

Fig. 2. TDS spectra for Ni (1) and alloy Ni–6.9%Al (2) were taken with heating rate of 5 K/s from samples annealed at 1070 K during 10 h after irradiation.

Table 1
The bubble parameters (mean size d and volume density ρ) in Ni and Ni–Al alloys

Post-irrad. annealing	Ni		Ni–4.2%Al		Ni–7.5%Al	
	d (nm)	ρ (m^{-3})	d (nm)	ρ (m^{-3})	d (nm)	ρ (m^{-3})
1 h at 920 K	8	$(3 \pm 1) \times 10^{22}$	5	$(6 \pm 2) \times 10^{22}$	2	$\sim 10^{24}$
10 h at 920 K	8.2	$\sim 10^{22}$	6	$(5 \pm 2) \times 10^{22}$	3	$\sim 10^{23}$
1 h at 1070 K	40	$(4 \pm 2) \times 10^{20}$	28.6	$(7 \pm 3) \times 10^{20}$	22.5	$(5 \pm 2) \times 10^{21}$
10 h at 1070 K	95	$(2 \pm 1) \times 10^{19}$	58	$(6 \pm 2) \times 10^{19}$	Fig. 3(b)[a]	
25 h at 1120 K	> 150[b], Fig. 3(c) and (d)	–	–	–	> 150[b]	–

[a]Large bubbles with $d > 100$ nm are located on the boundaries between γ'-phase particles and the matrix (see Fig. 3(b)).
[b]Pores penetrating the irradiated layer and crossing the sample surface (see Fig. 3(c) and (d)).

can be seen in Fig. 3(d) received in SEM, an opened porosity on the sample surface is observed.

Fig. 4 shows the changes of IF as a function of temperature for unirradiated Ni and alloy Ni–7.5%Al. The corresponding temperatures of main peaks are presented in Table 2. The observed peak temperatures on the low-temperature branch of the curves approximately coincide with those known in literature [15,16]. Besides, as well known [16], dopant elements shift significantly the IF peaks to higher temperatures. The effect especially is typical for grain boundary peaks that can be seen in Fig. 4 also.

The IF spectra for Ni and alloy Ni–7.5%Al taken from samples immediately after irradiation (experiment 1, curves I) and repeatedly after experiment 1 (experiment 2, curves II) are given in Figs. 5 and 6, respectively. The corresponding temperatures of main peaks are presented in Tables 3 and 4. These spectra contain a number of features (Tables 3 and 4, see also inserts in Figs. 5 and 6): (1). The additional peaks in Ni (peak 3) and in Ni–Al alloy (peak 4) occur as a result of the first heating (experiment 1), which were absent for unirradiated samples (see Fig. 4); the temperature of additional peak in Ni is in accordance with dissociation temperature for He–V complexes [6,17]. (2). The peaks caused by stress relaxation on the block boundaries shift to higher temperatures.

The repeated heating (experiment 2) causes the return of block boundary relaxation peak to initial (unirradiated) state, the intensification of peak corresponding to dissipation of energy on grain boundaries (it is quite possible due to grain boundary bubbles) and the occurrence of intensive peaks corresponding to dissipation of energy on dislocations decorated by helium bubbles (peaks 2 in Figs. 5 and 6).

Besides, as can be seen in Fig. 6, there are wealth of peaks in the irradiated alloy spectra at temperatures higher than 1050 K as in the case of the unirradiated alloy (Fig. 4). This can testify to their identical nature, that is, these peaks are caused by complex processes of reorganization of structure by formation of segregation and precipitation of the secondary γ'-phase (in the range

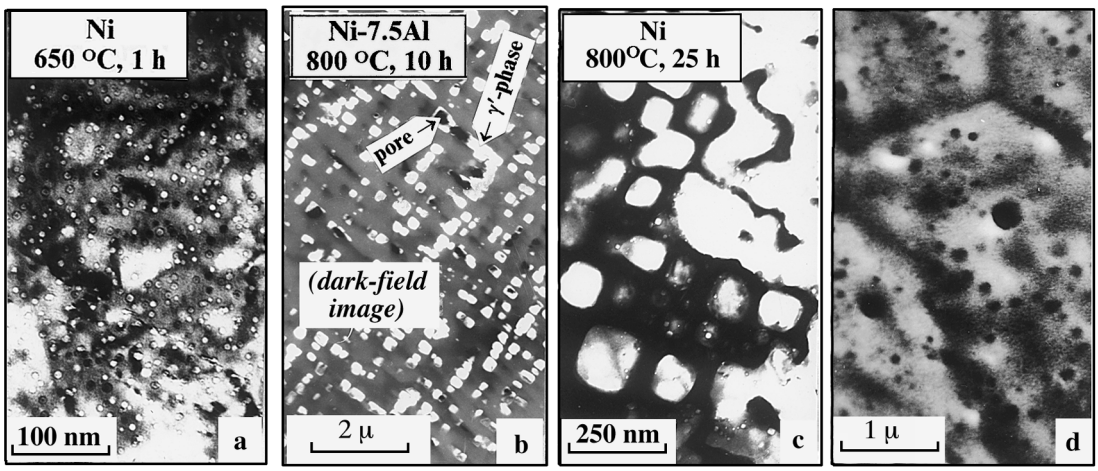

Fig. 3. Typical microstructure of Ni–Al alloys (obtained in TEM) after irradiation by He^+ ions and post-irradiation annealings up to 25 h at 920–1120 K. In (c) the network of the interconnected channels is visible; on (d) the surface of the same sample obtained by SEM.

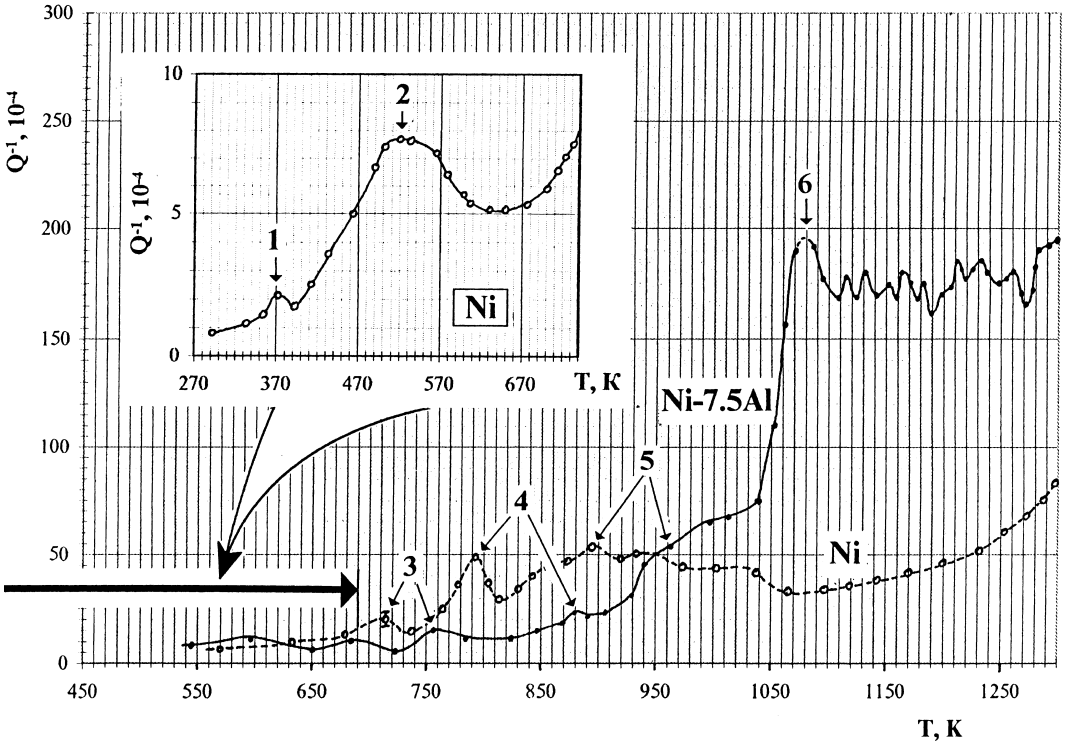

Fig. 4. The IF versus temperature for quenched unirradiated Ni and alloy Ni–7.5%Al obtained during uniform heating with heating rate of 4 K/min.

920–1120 K) and reverse dissolution of these objects with transition of alloying element atoms into the matrix (at temperatures higher than 1170 K) [2] etc.

4. Discussion

The presented data show a strong influence of aluminum on the helium behavior and bubble microstructure evolution process in nickel during post-irradiation heating. The atoms of Al occupy substitution positions in the crystal lattice of nickel, and having a significant size discrepancy with Ni atoms they create local deformation fields in a crystal (zones of compression). It is well known that such zones are areas for vacancies attraction, for example, induced by radiation. If the emergence centers of He_mV_n type complexes in pure Ni are usual vacancies (radiation-induced or structural, for example, quenched vacancies), so such centers could also be represented by substitution atoms in Ni–Al alloys because the areas of compression created by them "reserve" vacancies or their complexes which trap helium atoms during irradiation. In other words, the dopant atoms are centers for type $He_mAl_kV_n$ additional complexes in nickel. And at high concentration of helium or in the course of post-irradiation annealing they are the additional centers for bubble formation as can be seen in Table 1 and data [8,9,13,14].

Table 2
The temperatures of main peaks for unirradiated samples, K (to Fig. 4)

No.	Ni		Ni–7.5Al		Mechanisms	Refs. [15,16] (only for Ni)
	The range	T_m	The range	T_m		
1	350–390	370	–	–	Magnetic transformation	360–370
2	390–610	520	–	–	Dissipation of energy on impurities	520–610
3	690–730	715	730–780	755	–	–
4	750–810	790	870–920	880	Grain boundaries	670–770
5	870–920	895	930–1000	960	Stress relaxation on the block boundaries	900–990
6	–	–	1040–1110	1080	Segregation of n · Al	–

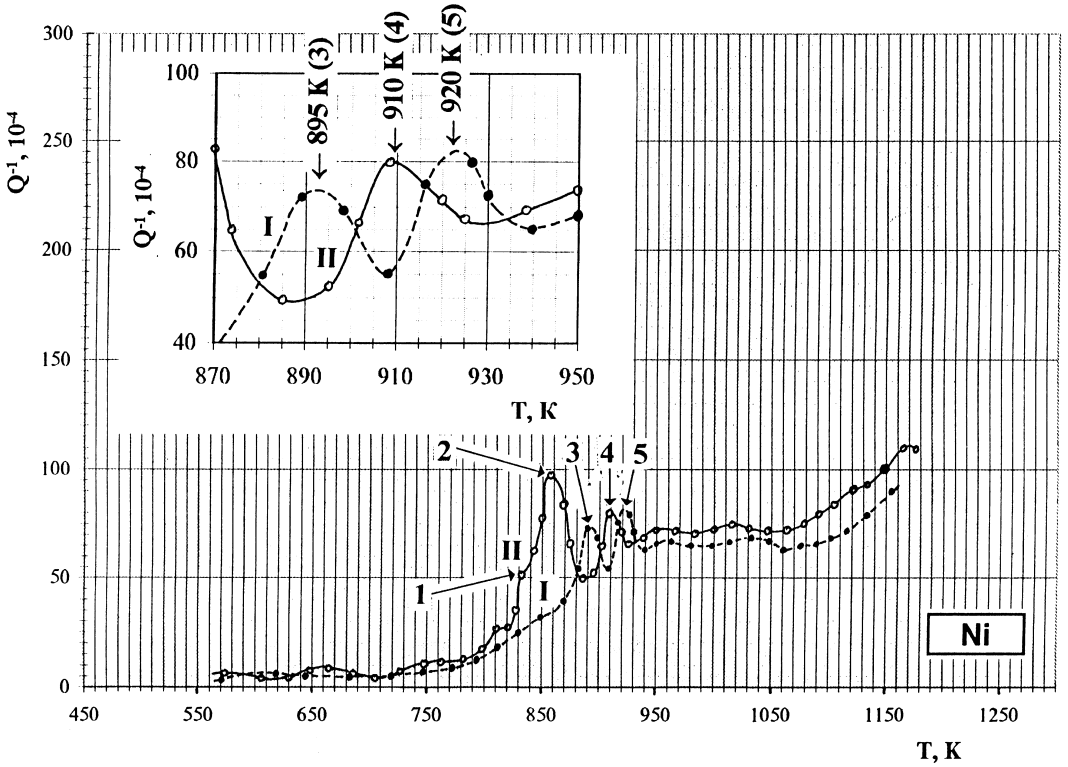

Fig. 5. The IF change as a function of temperature for Ni irradiated by He^+-ions: I – the first heating (experiment 1) and II – the second heating after experiment 1 (experiment 2) with heating rate of 4 K/min. The peaks occurring due to irradiation are presented on the insert.

It could result in increase of the forming complexes density (complexes He_mV_n + $He_mAl_kV_n$). Moreover, the complexes of $He_mAl_kV_n$ type can be thermally more stable than complexes of He_mV_n type in nickel (they must dissociate at temperature before 920 K according to [6,9,18]), because, as can be seen in Figs. 1 and 2, these alloys contain considerably more quantity of helium than pure nickel after long-time annealing at 1020 and 1070 K. In pure Ni the release of significant quantity of helium occurring during isothermal post-irradiation annealing at 1020 and 1070 K can be explained by dissociation of He_mV_n complexes and migration of a part of the liberated helium atoms to the surface, because as shown in [6,17] at temperatures above the complex dissociation temperature the helium atoms are able to migrate in and beyond the implanted zone by mechanism similar to the 'classical' dissociative diffusion which plays an increasingly prominent role in gas migration with growing temperature. The decrease of the helium quantity, held in the decomposing alloys (N_{Al} > 5%), is due to the release of gas from large bubbles aligning on the incoherent boundaries between γ'-precipitates and the matrix, the bubbles intersecting the sample surface during their growth (Fig. 3(b)).

The increase of annealing time at 1070 K or increase of annealing temperature to 1120 K result in the alignment of the remaining gas concentration in samples. This supports the assumption made in [8,9,13] that the

Table 3
The temperatures of the main peaks for irradiated Ni, K (to Fig. 5)

No.	1st heating		2nd heating		Mechanisms
	The range	T_m	The range	T_m	
1	–	–	820–860	835	Grain boundaries
2	–	–	845–885	855	Dissipation of energy on dislocations
3	870–910	895	–	–	Dissociation of He_mV_n complexes
4	–	–	885–930	910	Dissipation of energy on the block boundaries
5	910–940	920	–	–	

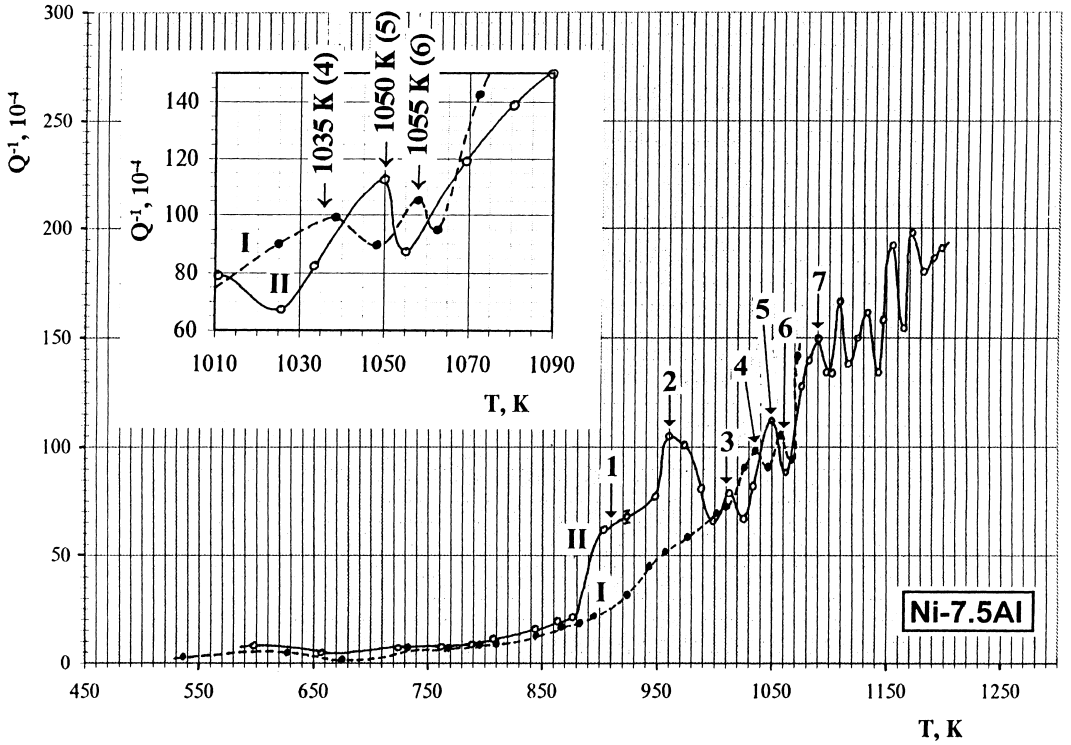

Fig. 6. The IF change as a function of temperature for alloy Ni–7.5%Al irradiated by He^+-ions: I – the first heating (experiment 1) and II – the second heating after experiment 1 (experiment 2) with heating rate of 4 K/min. The peaks occurring due to irradiation are presented on the insert.

mechanism of helium delay in the alloys is its preservation in the complexes containing atoms of alloying elements; in so doing, the dissociation temperature of such complexes should be, at least, not lower than 1020 K, as exemplified by data presented in Fig. 6 and Table 4. Besides the additional peaks found out in the IF spectra during primary heating, which were caused by introduction of helium (peaks 3 and 4 in Figs. 5 and 6, respectively), can be attributed to complexes of He_mV_n type in nickel (Fig. 5) and to complexes of $He_mAl_kV_n$ type in the alloy (Fig. 6). The additional peak in Ni is located at 870–910 K (Table 3), that corresponds to the dissociation temperature of the most stable complexes in nickel [6,18]. By this analogy we believe that the additional peak in the Ni–7.5%Al alloy is caused by dissociation of type $He_mAl_kV_n$ complexes. In such a case, the temperature of their dissociation is in the 1010–1045 K temperature range (Table 4).

5. Conclusions

Thus, the experimental results obtained on the influence of alloying on ion-implanted helium behavior and on bubble microstructure parameters in nickel have shown that:

Table 4
The temperatures of the main peaks for irradiated Ni–7.5Al alloy, K (to Fig. 6)

No.	1st heating		2nd heating		Mechanisms
	The range	T_m	The range	T_m	
1	–	–	880–960	910	Grain boundaries
2	–	–	940–1000	960	Dissipation of energy on dislocations
3	–	–	1000–1025	1010	Segregation of n · Al
4	1010–1045	1035	–	–	Dissociation of $He_mAl_kV_n$ complexes
5	–	–	1025–1055	1050	Dissipation of energy on the block boundaries
6	1045–1065	1055	–	–	
7	–	–	1060–1100	1090	Decomposition of γ'-Ni_3Al

1. The substitution atoms (aluminum) increase the density of forming helium bubbles and reduce their sizes in nickel. Two systems of bubbles are formed in decomposing alloys as a result of long-time post-irradiation annealing: fine bubbles located in the matrix, and large ones connected with particles of the secondary γ'-phase.
2. The helium remaining in Ni–Al solid solutions is much more than in pure nickel and decomposing alloys ($N_{Al} > 5\%$), after isothermal long-time post-irradiation annealing at 1020 K for 25 h and 1070 K for 10 h.
3. The measurement of internal friction of irradiated alloys supplements the TDS and TEM data on possibility of $He_mAl_kV_n$ complicated complexes formation in Ni–Al alloys.
4. It has been confirmed that thermally more stable complexes of $He_mAl_kV_n$ type containing dopant element atoms can be formed in alloys alongside with usual complexes of He_mV_n type. The presence of $He_mAl_kV_n$ complexes, which are stable at least up to 1020 K, explains the phenomena found.

References

[1] B.A. Kalin, D.M. Skorov, V.L. Yakushin, The Problems in the Fusion Reactor Materials Choosing, Energoatomizdat, Moscow, 1985.
[2] N.M. Beskorovainy, B.A. Kalin, P.A. Platonov, I.I. Chernov, Structural Materials for Nuclear Reactors, Energoatomizdat, Moscow, 1995.
[3] H. Schroeder, W. Kesternich, H. Ullmaier, Nucl. Eng. Design/Fusion 2 (1985) 65.
[4] V.F. Zelensky, I.M. Nekludov, T.P. Chernyaeva, Radiation Defects and Swelling of Materials, Naukova Dumka, Kiev, 1988.
[5] H. Schroeder, U. Stamm, Proceedings of 14th Symposium on Effects of Radiat. on Mater., ASTM STR 1046, 1989, p. 223.
[6] V.N. Chernikov, A.P. Zakharov, P.R. Kazansky, J. Nucl. Mater. 155/157 (1988) 1142.
[7] H. Ullmaier, Nucl. Fusion 24 (1984) 1039.
[8] B.A. Kalin, I.I. Chernov, A.N. Kalashnikov, B.G. Solovyev, Proceedings of 17th Symposium on Effects of Radiat. on Mater., ASTM STR 1270, 1996, p. 1013.
[9] B.A. Kalin, I.I. Chernov, A.N. Kalashnikov, B.G. Solovyev, Plasma Devices Operations 4 (1996) 313.
[10] A.N. Kalashnikov, B.A. Kalin, I.V. Reutov et al., Phys. Met. Met. Sci. 7 (1990) 203 (in Russian).
[11] B.A. Kalin, A.V. Markin, A.A. Volkov et al., Atomic Energy 59 (1985) 150 (in Russian).
[12] B.A. Kalin, I.I. Chernov, A.N. Kalashnikov, M.N. Esaulov, The Problems of Atomic Sci. Technics. Ser.: Radiat. Damage Phys. Radiat. Mater. Sci. 1(65)/2(66) (1999) 53 (in Russian).
[13] B.A. Kalin, I.I. Chernov, A.N. Kalashnikov, V.V. Timofeyev, J. Nucl. Mater. 233–237 (1996) 1142.
[14] B.A. Kalin, I.I. Chernov, A.N. Kalashnikov et al., Proceedings of 16th Symposium on Effects of Radiat. on Mater., ASTM STR 1175, 1994, p. 838.
[15] V.S. Postnikov, Internal Friction in Metals, Metallurgiya, Moscow, 1974.
[16] H. Gleiter, B. Chalmers, High-Angle Grain Boundaries, Pergamon, New York, 1972.
[17] V. Phillips, S. Sonnenberg, J.M. Williams, J. Nucl. Mater. 107 (1982) 271.
[18] V.N. Chernikov, H. Trinkaus, P. Jung, H. Ullmaier, J. Nucl. Mater. 170 (1990) 31.